Preprints of the 19th World Congress
The International Federation of Automatic Control
Cape Town, South Africa. August 24-29, 2014

Nonlinear Burn Control in Tokamak Fusion Reactors via Output Feedback ⋆

Mark D. Boyer *, **Eugenio Schuster** *

* *Mechanical Engineering and Mechanics, Lehigh University, Bethlehem, PA 18015, USA.*

Abstract: The next experimental step in the development of nuclear fusion reactors is the ITER tokamak. It is designed to explore the burning plasma regime in which the plasma temperature is sustained mostly by self-heating from fusion reactions. Burn control, the control of fusion power and other reactor parameters through modulation of fueling and heating, will be essential for achieving and maintaining desired operating points and ensuring stability. Design of burn control strategies is made challenging by the multi-variable, highly nonlinear, uncertain nature of the system. Furthermore, due to the extreme conditions in fusion reactors, diagnostic systems may be limited. To deal with these challenges, we propose the use of a nonlinear, multi-variable output feedback control strategy with a proportional-integral observer. A simulation study is carried out to illustrate the performance of the scheme using a set of diagnostics likely to be available in ITER.

Keywords: Nonlinear Control Systems, Nuclear Reactors, Lyapunov Stability, Output Feedback, Uncertain Dynamic Systems.

1. INTRODUCTION

For nuclear fusion to become an economical means of producing power, tokamak reactors must achieve a burning plasma characterized by a large ratio of fusion power to external heating power. Precise control of the plasma density and temperature will be required to ensure good transient performance when moving between operating points, and to respond to unexpected changes in confinement, impurity content, or other parameters. Feedback control will also be critical for enabling operation at thermally unstable points. Without a well-designed burn control scheme, disruptive plasma instabilities could be triggered, stopping operation and potentially damaging the machine.

Modulation of the burn condition is made challenging by the nonlinearly coupled, multi-variable, uncertain nature of the burning plasma system. In past work on the problem of burn control, the feasibility of various actuators has been studied (Mandrekas and Stacey, 1989; Haney et al., 1990). Most previous efforts made use of just one of the available actuators and linearized the system model to make use of linear control design techniques. In Leonov et al. (2005), a diagonal multi-input, multi-output linear control scheme was developed, while non-model-based proportional-integral controllers were studied in (Mitarai, 2002; Mitarai et al., 2010). When tested using nonlinear models, these control strategies succeed in stabilizing the system against a limited set of perturbations and are only valid near the operating point for which they are designed. In our previous work, Schuster et al. (2003); Boyer and Schuster (2011, 2012), a zero-dimensional nonlinear model for the energy and the ion density dynamics was used to synthesize nonlinear feedback controllers for stabilizing the burn condition. The controllers utilize auxiliary power modulation, controlled impurity injection, and fueling modulation as actuators simultaneously. Nonlinear burn control using multiple actuators had only been done previously in works using non-model-based techniques, like neural networks (Vitela, 2001).

Due to the extreme conditions in fusion reactors, as well as cost considerations, diagnostic systems may be limited. Because the proposed nonlinear burn control control approach relies on knowledge of the states of the system (state feedback), it may not be directly implementable. To overcome this, a dynamic observer that combines knowledge from the mathematical model of the system with the available real-time output measurements to estimate the system states will likely be necessary. In this work, we design a nonlinear proportional-integral observer (PIO) to augment the nonlinear controller design, resulting in an output feedback control scheme. PIO designs differ from classical observers by the presence of an integral component in the output injection term, which provides an additional degree of freedom that can be used to decrease sensitivity to model uncertainties and disturbances. Output feedback controllers with PIOs have been proposed for general linear systems (Beale and Shafai, 1989) and have been applied to certain nonlinear systems (Jung et al., 2007; Orjuela et al., 2008). For the nominal system, the observer design proposed in this work is stable for suitably small state estimation errors or observer gains. The state estimation error is input-to-state-stable (ISS) with respect to a particular set of uncertain model parameters, while, due to the inclusion of integral output injection terms, the output estimation error converges to zero asymptotically.

⋆ This work was supported by the US Department of Energy (DE-SC0001334, DE-SC0010661). E-mail contact of first author: m.dan.boyer@lehigh.edu.

This paper is organized as follows. The model used for control design is given in Section 2. The design of a nonlinear multi-variable controller and observer is detailed in Section 3, and a simulation study is shown in 4. Finally, conclusions and future work are discussed in 5.

2. BURNING PLASMA MODEL

We consider a burning plasma model of the form

$$\dot{n}_\alpha = -\theta_1 \frac{n_\alpha}{\tau_E^{sc}} + S_\alpha, \quad (1)$$

$$\dot{E} = -\theta_2 \frac{E}{\tau_E^{sc}} + P_\alpha - P_{rad} + P_{aux} + P_{Ohm}, \quad (2)$$

$$\dot{n}_{I,c} = -\theta_7 \frac{n_{I,c}}{\tau_E^{sc}} + S_I^{inj}, \quad (3)$$

$$\dot{n}_{I,sp} = -\theta_7 \frac{n_{I,sp}}{\tau_E^{sc}} + S_I^{sp}, \quad (4)$$

$$\dot{n}_D = -\theta_3 \frac{n_D}{\tau_E^{sc}} + \theta_4 \frac{n_T}{\tau_E^{sc}} - S_\alpha + S_D^{inj}, \quad (5)$$

$$\dot{n}_T = \theta_5 \frac{n_D}{\tau_E^{sc}} - \theta_6 \frac{n_T}{\tau_E^{sc}} - S_\alpha + S_T^{inj}, \quad (6)$$

where n_α, n_D, n_T, and E are the α-particle, deuterium, tritium, and energy densities, respectively. The deuterium and tritium injection rates (controller inputs) are given by S_D^{inj} and S_T^{inj}. Note that the second term in (5) and first term in (6) arise due to coupling caused by particles recycling from the walls of the reactor. The term $n_{I,c}$ represents the density of impurities due to controlled impurity injection, while $n_{I,sp}$ represents the uncontrolled impurity density that arises due to sputtering from plasma facing components of the confinement vessel. The source of α-particles from fusion is given by

$$S_\alpha = \gamma(1-\gamma)\, n_{DT}^2 \langle \sigma v \rangle,\ n_{DT} = n_D + n_T,\ \gamma = \frac{n_T}{n_{DT}}, \quad (7)$$

where $n_{DT} = n_D + n_T$ is the density of deuterium-tritium fuel and γ is the tritium fraction. The DT reactivity $\langle \sigma\nu \rangle$, a highly nonlinear, positive and bounded function of the plasma temperature, $T = \frac{2}{3}\frac{E}{n}$, is calculated by

$$\langle \sigma\nu \rangle = exp\left(\frac{a}{Tr} + a_2 + a_3 T + a_4 T^2 + a_5 T^3 + a_6 T^4\right), \quad (8)$$

where the parameters a_i and r are taken from Hively (1977). The plasma density is given by

$$n = 2n_D + 2n_T + 3n_\alpha + (Z_I + 1)\, n_I. \quad (9)$$

The term S_I^{inj} (controller input) is the injection of impurities that increases the controlled impurity density $n_{I,c}$ to cool the plasma. The sputtering source is modeled as

$$S_I^{sp} = \frac{f_I^{sp} n}{\tau_I^*} + f_I^{sp} \dot{n}, \quad (10)$$

where $0 \le f_I^{sp} \ll 1$ in order to maintain $n_{I,sp} = f_I^{sp} n$. This simple model reflects the fact that there is typically a small uncontrolled impurity content. To simplify presentation, we consider both impurity populations to have the same atomic number Z_I. The total impurity content $n_I = n_{I,s} + n_{I,c}$ is then governed by

$$\dot{n}_I = -\theta_7 \frac{n_I}{\tau_E^{sc}} + S_I^{inj} + S_I^{sp}. \quad (11)$$

P_{aux} (controller input) is the auxiliary heating power, while $P_\alpha = Q_\alpha S_\alpha$ is the plasma heating from fusion where $Q_\alpha = 3.52$ MeV is the energy of α-particles. P_{rad} represents radiative cooling losses, which are approximated by an expression for bremsstrahlung losses (Stacey, 2010),

$$P_{rad} = A_{brem}\left(n_D + n_T + 4n_\alpha + Z_I^2 n_I\right) n_e \sqrt{T(keV)}, \quad (12)$$

where A_{brem} is a constant and n_e is the electron density. The electron density is obtained from the neutrality condition $n_e = n_D + n_T + 2n_\alpha + Z_I n_I$. Ohmic heating P_{Ohm} is approximated as (Stacey, 2010)

$$P_{Ohm} = 2.8 \times 10^{-9} Z_{eff} I_p^2 a^{-4} T^{-3/2}, \quad (13)$$

where I_p is in Amps, T is in keV, and $Z_{eff} = \left(n_D + n_T + 4n_\alpha + n_I Z_I^2\right)/n_e$.

The state-dependent energy confinement time is given by

$$\tau_E^{sc} = 0.0562 I_p^{0.93} B_T^{0.15} P^{-0.69} n_{e19}^{0.41} M^{0.19} R^{1.97} \epsilon^{0.58} \kappa_{95}^{0.78}, \quad (14)$$

where $P = P_{aux} + P_{Ohm} + P_\alpha - P_{rad}$ is the total power (MW), n_{e19} is the electron density ($10^{19}\mathrm{m}^{-3}$), M is the effective mass of the plasma (amu) (ITER Director, 2001). Based on ITER design parameters, we consider the plasma current $I_p = 15.0$ MA, the toroidal magnetic field $B_T = 5.3$ T, the major radius $R = 6.2$ m, and the elongation at the 95% flux surface $\kappa_{95} = 1.7$. A minor radius $a = 2.0$ m is used to calculate the aspect ratio $\epsilon = a/R$.

The terms θ_i for $i \in \{1, ..., 7\}$ represent model parameters that depend on the confinement and particle recycling properties of the machine. In the control design, we consider them to be uncertain and bounded.

3. NONLINEAR CONTROLLER AND OBSERVER

We consider an observer of the form

$$\dot{\mathring{n}}_\alpha = -\hat{\theta}_1 \frac{\mathring{n}_\alpha}{\tau_E^{sc}} + S_\alpha + L_\alpha, \quad (15)$$

$$\dot{\mathring{E}} = -\hat{\theta}_2 \frac{\mathring{E}}{\tau_E^{sc}} + P_\alpha - P_{rad} + P_{aux} + P_{Ohm} + L_E, \quad (16)$$

$$\dot{\mathring{n}}_I = -\hat{\theta}_7 \frac{\mathring{n}_I}{\tau_E^{sc}} + S_I^{inj} + S_I^{sp} + L_I, \quad (17)$$

$$\dot{\mathring{n}}_D = -\hat{\theta}_3 \frac{\mathring{n}_D}{\tau_E^{sc}} + \hat{\theta}_4 \frac{\mathring{n}_T}{\tau_E^{sc}} - S_\alpha + S_D^{inj} + L_D, \quad (18)$$

$$\dot{\mathring{n}}_T = \hat{\theta}_5 \frac{\mathring{n}_D}{\tau_E^{sc}} - \hat{\theta}_6 \frac{\mathring{n}_T}{\tau_E^{sc}} - S_\alpha + S_T^{inj} + L_T, \quad (19)$$

where L_α, L_E, L_I, L_D, and L_T are to-be-designed output injection terms. The terms S_α, P_α, P_{rad}, P_{Ohm}, and S_I^{sp} are considered to be measured, based on the diagnostic systems planned for ITER (Snipes et al., 2012) (if unavailable, these terms could always be estimated based on the observer state estimates). The terms $\hat{\theta}_i$ for $i \in \{1, \ldots, 7\}$ are estimates of the uncertain model parameters. The measured output map is considered to be of the form

$$y = h(n_\alpha, E, n_I, n_D, n_T). \quad (20)$$

We consider an additional state, $\check{z}$, governed by

$$\dot{\check{z}} = \mathring{y} - y = \check{y}, \quad (21)$$

where $\mathring{y} = h(\mathring{n}_\alpha, \mathring{E}, \mathring{n}_I, \mathring{n}_D, \mathring{n}_T)$.

For the purposes of control design, we consider the estimated states $\mathring{n}$ and $\mathring{\gamma}$, which are governed by

$$\begin{aligned}\dot{\mathring{n}} =&2\left[\left(\hat{\theta}_5-\hat{\theta}_3\right)\frac{\mathring{n}_D}{\tau_E^{sc}}+\left(\hat{\theta}_4-\hat{\theta}_6\right)\frac{\mathring{n}_T}{\tau_E^{sc}}-2S_\alpha+S_D^{inj}+S_T^{inj}\right.\\&\left.+L_D+L_T\right]+3\left[-\hat{\theta}_1\frac{\mathring{n}_\alpha}{\tau_E^{sc}}+S_\alpha+L_\alpha\right]\\&+(Z_I+1)\left[-\hat{\theta}_7\frac{\mathring{n}_I}{\tau_E^{sc}}+S_I^{inj}+S_I^{sp}+L_I\right],\end{aligned}\tag{22}$$

$$\begin{aligned}\dot{\mathring{\gamma}} =&\frac{1}{\mathring{n}_{DT}}\left\{\hat{\theta}_5\frac{\mathring{n}_D}{\tau_E^{sc}}-\hat{\theta}_6\frac{\mathring{n}_T}{\tau_E^{sc}}-S_\alpha+S_T^{inj}+L_T\right.\\&-\mathring{\gamma}\left[\left(\hat{\theta}_5-\hat{\theta}_3\right)\frac{\mathring{n}_D}{\tau_E^{sc}}+\left(\hat{\theta}_4-\hat{\theta}_6\right)\frac{\mathring{n}_T}{\tau_E^{sc}}-2S_\alpha+S_D^{inj}\right]\\&\left.+S_T^{inj}+L_D+L_T\right]\Bigg\}.\end{aligned}\tag{23}$$

We define the tracking errors $\tilde{E}=\mathring{E}-E^r$, $\tilde{\gamma}=\mathring{\gamma}-\gamma^r$, and $\tilde{n}=\mathring{n}-n^r$ to write

$$\begin{aligned}\dot{\tilde{E}} =&-\hat{\theta}_2\frac{\tilde{E}}{\tau_E^{sc}}-\hat{\theta}_2\frac{E^r}{\tau_E^{sc}}+P_\alpha-P_{rad}+P_{aux}\\&+P_{Ohm}+L_E-\dot{E}^r,\end{aligned}\tag{24}$$

$$\dot{\tilde{\gamma}}=-\hat{\theta}_6\frac{\tilde{\gamma}}{\tau_E^{sc}}+\frac{2\left[u(\gamma^r)+(1-\mathring{\gamma})S_T^{inj}-\mathring{\gamma}S_D^{inj}\right]}{\mathring{n}-3\mathring{n}_\alpha-(Z_I+1)\mathring{n}_I},\tag{25}$$

$$\begin{aligned}\dot{\tilde{n}} =&-\tilde{n}\left[-\left(\hat{\theta}_5-\hat{\theta}_3\right)\frac{(1-\mathring{\gamma})}{\tau_E^{sc}}-\left(\hat{\theta}_4-\hat{\theta}_6\right)\frac{\mathring{\gamma}}{\tau_E^{sc}}\right]\\&+v-\dot{n}^r+2\left(S_D^{inj}+S_T^{inj}\right),\end{aligned}\tag{26}$$

where

$$\begin{aligned}u(\gamma^r)=&\frac{\mathring{n}-3\mathring{n}_\alpha-(Z_I+1)\mathring{n}_I}{2}\left[\hat{\theta}_5\frac{(1-\mathring{\gamma})}{\tau_E^{sc}}-\hat{\theta}_6\frac{\gamma^r}{\tau_E^{sc}}-\dot{\gamma}^r\right.\\&\left.-\left(\hat{\theta}_5-\hat{\theta}_3\right)\frac{\left(\mathring{\gamma}-\mathring{\gamma}^2\right)}{\tau_E^{sc}}-\left(\hat{\theta}_4-\hat{\theta}_6\right)\frac{\mathring{\gamma}^2}{\tau_E^{sc}}\right]\\&+(2\mathring{\gamma}-1)S_\alpha+(1-\mathring{\gamma})L_T-\mathring{\gamma}L_D,\end{aligned}\tag{27}$$

$$\begin{aligned}v=&\left[-n^r+3\mathring{n}_\alpha+(Z_I+1)\mathring{n}_I\right]\left[-\left(\hat{\theta}_5-\hat{\theta}_3\right)\frac{(1-\mathring{\gamma})}{\tau_E^{sc}}\right.\\&\left.-\left(\hat{\theta}_4-\hat{\theta}_6\right)\frac{\mathring{\gamma}}{\tau_E^{sc}}\right]-4S_\alpha+3\left[-\hat{\theta}_1\frac{\mathring{n}_\alpha}{\tau_E^{sc}}+S_\alpha+L_\alpha\right]\\&+(Z_I+1)\left[-\hat{\theta}_7\frac{\mathring{n}_I}{\tau_E^{sc}}+S_I^{inj}+S_I^{sp}+L_I\right]\\&+2(L_D+L_T).\end{aligned}\tag{28}$$

Note that, without steady-state controlled impurity injection, the reference $r=[E^r,n^r,\gamma^r]$ uniquely determines the equilibrium values of n_α and n_I, and these states remain bounded if r is stabilized. We therefore make regulation of r the objective of the control design.

3.1 Controller Design

The error $\tilde{E}$ can be driven to zero by satisfying

$$\begin{aligned}f(n,E,n_\alpha,n_I,\gamma)=&-\hat{\theta}_2\frac{E^r}{\tau_E^{sc}}+P_{Ohm}+P_\alpha-P_{rad}+P_{aux}\\&+L_E-\dot{E}^r+K_E\tilde{E}=0.\end{aligned}\tag{29}$$

The condition (29) can be satisfied in several different ways. The auxiliary heating term P_{aux} enters directly, the actuators S_D^{inj} and S_T^{inj} can be used to change P_α by modulating the tritium fraction, and the impurity injection term S_I^{inj} can be used to increase impurity content and consequently P_{rad}. Having several methods available enables us to achieve stabilization despite saturation of one or even several of the available actuators.

Step 1: We first calculate P_{aux} as

$$\begin{aligned}P_{aux}^{unsat}=&\hat{\theta}_2\frac{E^r}{\tau_E^{sc}}-\gamma^r(1-\gamma^r)\frac{P_\alpha}{\mathring{\gamma}(1-\mathring{\gamma})}+P_{rad}\\&-P_{Ohm}-L_E+\dot{E}^r-K_E\tilde{E},\end{aligned}\tag{30}$$

where $P_\alpha/\left[\mathring{\gamma}(1-\mathring{\gamma})\right]$ is an estimate of $Q_\alpha n_{DT}^2\langle\sigma\nu\rangle$. This value is saturated by the limits P_{aux}^{max}, which depends on the installed power on the tokamak, and $P_{aux}^{min}\geq 0$, which depends on the operating scenario.

Step 2: We next find a trajectory γ^* that would result in a fusion heating value satisfying (29), i.e.

$$\begin{aligned}\gamma^*(1-\gamma^*)\frac{P_\alpha}{\mathring{\gamma}(1-\mathring{\gamma})}=&P_{rad}-P_{Ohm}-P_{aux}-L_E\\&+\hat{\theta}_2\frac{E^r}{\tau_E^{sc}}+\dot{E}^r-K_E\tilde{E}.\end{aligned}\tag{31}$$

Solving this equation yields

$$\begin{aligned}\gamma^*(1-\gamma^*)=&\frac{\mathring{\gamma}(1-\mathring{\gamma})}{P_\alpha}\left[\hat{\theta}_2\frac{E^r}{\tau_E^{sc}}+P_{rad}-P_{Ohm}-P_{aux}\right.\\&\left.-L_E+\dot{E}^r-K_E\tilde{E}\right]=C,\end{aligned}\tag{32}$$

$$\gamma^*=\frac{1\pm\sqrt{1-4C}}{2}.\tag{33}$$

Note that, if the value of P_{aux} calculated in Step 1 is not saturated, then $\gamma^*=\gamma^r$. This can be shown by substituting (30) into (29). If $C\leq 0.25$, the two resulting solutions for γ^* are real and we take the tritium-lean solution, such that $\gamma^*\leq 0.5$. If $C\geq 0.25$, even the optimal isotopic mix and maximum value of auxiliary heating will not generate enough heating to satisfy $f=0$, indicating that the requested operating point may not be achievable for the amount of auxiliary heating power installed on the device. Barring this situation, we have that

$$f(n,E,n_\alpha,n_I,\gamma^*)=0.\tag{34}$$

This allows us to write $f=\hat{\gamma}\phi_\gamma$ where $\hat{\gamma}=\mathring{\gamma}-\gamma^*$ and ϕ_γ is a continuous function. Noting (24) and (29), we can then write the dynamics of the energy perturbation as

$$\dot{\tilde{E}}=-\hat{\theta}_2\frac{\tilde{E}}{\tau_E^{sc}}-K_E\tilde{E}+\hat{\gamma}\phi_\gamma,\tag{35}$$

while the dynamics of $\hat{\gamma}$ can be written as

$$\dot{\hat{\gamma}}=-\hat{\theta}_6\frac{\hat{\gamma}}{\tau_E^{sc}}+\frac{2\left[u(\gamma^*)+(1-\mathring{\gamma})S_T^{inj}-\mathring{\gamma}S_D^{inj}\right]}{\mathring{n}-3\mathring{n}_\alpha-(Z_I+1)\mathring{n}_I}.\tag{36}$$

by noting (25) and (27).

Step 3: Having selected P_{aux} and γ^* in, we next choose S_D^{inj} and S_T^{inj} to ensure that $\tilde{E}$, $\hat{\gamma}$, and $\tilde{n}$, governed by (35), (36), and (26), are driven to zero. We consider the Lyapunov function $V_0=V_n+V_{E,\gamma}$ where $V_n=\frac{1}{2}\tilde{n}^2$ and $V_{E,\gamma}=\frac{1}{2}k_1\tilde{E}^2+\frac{1}{2}\hat{\gamma}^2$. It can be shown that satisfying

$$2\left(S_T^{inj}+S_D^{inj}\right)=-v-K_n\tilde{n}+\dot{n}^r,\tag{37}$$

$$\begin{aligned}(1-\mathring{\gamma})S_T^{inj}-\mathring{\gamma}S_D^{inj}=&-\frac{\mathring{n}-3\mathring{n}_\alpha-(Z_I+1)\mathring{n}_I}{2}\\&\times\left(k_1\tilde{E}\phi_\gamma+K_\gamma\hat{\gamma}\right)-u(\gamma^*),\end{aligned}\tag{38}$$

where $K_n > 0$ and $K_\gamma > 0$ results in

$$\dot{V}_n = -\tilde{n}^2 \left(-\left(\hat{\theta}_5 - \hat{\theta}_3\right) \frac{(1-\mathring{\gamma})}{\tau_E^{sc}} - \left(\hat{\theta}_4 - \hat{\theta}_6\right) \frac{\mathring{\gamma}}{\tau_E^{sc}} + K_n \right) < 0, \quad (39)$$

$$\dot{V}_{E,\gamma} = -k_1 \hat{\theta}_2 \frac{\tilde{E}^2}{\tau_E^{sc}} - k_1 K_E \tilde{E}^2 - \left(\frac{1}{\tau_T} + K_\gamma \right) \hat{\gamma}^2 < 0, \quad (40)$$

such that $\dot{V}_0 < 0$, guaranteeing asymptotic stability of the system (for physically relevant parameters, $\theta_5 < \theta_3$ and $\theta_4 < \theta_6$). The conditions (37) and (38) can be satisfied by

$$S_D^{inj} = \frac{\mathring{n} - 3\mathring{n}_\alpha - (Z_I+1)\mathring{n}_I}{2} \left(k_1 \tilde{E} \phi_\gamma + K_\gamma \hat{\gamma} \right) + u(\gamma^*) + (1-\mathring{\gamma}) \left(\frac{-v - K_n \tilde{n} + \dot{n}^r}{2} \right), \quad (41)$$

$$S_T^{inj} = \left(\frac{-v - K_n \tilde{n} + \dot{n}^r}{2} \right) - S_D^{inj}. \quad (42)$$

These values are subject to the constraints $0 \leq S_D^{inj} \leq S_D^{inj,max}$ and $0 \leq S_T^{inj} \leq S_T^{inj,max}$. If one of the fueling actuators saturates, we cannot satisfy both conditions of the control law, so we must choose to either control $\mathring{n}$ or $\mathring{\gamma}$. To avoid a potential violation of the disruptive density limit, we instead choose to maintain control of the density by satisfying (37).

Due to fueling saturation, we may have $\dot{V}_{E,\gamma} > 0$, that is, stability of the system may not be ensured with the previously considered actuators. There are two situations to consider, either a quench or an excursion. In a quench, the controller has already increased heating to its maximum, so the only alternative would be to alter magnetic parameters to improve confinement (see (14)) or to change the target operating point to an achievable one. In an excursion, however, we can use impurity injection to stabilize the energy, despite the heating and fueling saturation. In this case we enable the use of impurity injection by setting the flag $F_{imp} = 1$ and proceeding to Step 4.

Step 4: If $F_{imp} = 1$, we use the expression for radiation losses given in (12) to find an impurity density n_I^* that satisfies condition (29). Defining the error $\hat{n}_I = \mathring{n}_I - n_I^*$, we can write its dynamics as

$$\dot{\hat{n}}_I = -\hat{\theta}_7 \frac{\hat{n}_I}{\tau_E^{sc}} - \hat{\theta}_7 \frac{n_I^*}{\tau_E^{sc}} + S_I^{inj} + S_I^{sp} - \dot{n}_I^*. \quad (43)$$

Based on the choice of n_I^*, we have that

$$f(n, E, n_\alpha, \gamma, n_I^*) = 0, \quad (44)$$

which allows us to write $f = \hat{n}_I \phi_I$ where ϕ_I is a continuous function. We can then rewrite (24) as

$$\dot{\tilde{E}} = -\hat{\theta}_2 \frac{\tilde{E}}{\tau_E^{sc}} - K_E \tilde{E} + \hat{n}_I \phi_I. \quad (45)$$

We take as a Lyapunov function $V_1 = V_n + V_\gamma + V_{E,I}$ where $V_\gamma = \frac{1}{2}\hat{\gamma}^2$ and $V_{E,I} = \frac{1}{2}k_3 \tilde{E}^2 + \frac{1}{2}\hat{n}_I^2$. By satisfying

$$S_I^{inj} = -k_3 \tilde{E} \phi_I + \hat{\theta}_7 \frac{n_I^*}{\tau_E^{sc}} - S_I^{sp} + \dot{n}_I^* - K_I \hat{n}_I, \quad (46)$$

where $K_I > 0$, the derivative of $V_{E,I}$ can be reduced to

$$\dot{V}_{E,I} = -k_3 \hat{\theta}_2 \frac{\tilde{E}^2}{\tau_E^{sc}} - k_3 K_E \tilde{E}^2 - K_I \hat{n}_I^2 < 0. \quad (47)$$

We modify the tritium fraction trajectory to $\gamma^* = \gamma^*_{(\text{Step 2})} - K_S \int_{t_0}^t S_I^{inj} dt$ where $\gamma^*_{(\text{Step 2})}$ is the value of γ^* calculated in Step 2, $K_S > 0$, and t_0 is the time at which impurity injection was first used. This ensures that the tritium fraction is, if possible, eventually reduced to such a level that impurity injection is no longer needed, i.e., $S_I^{inj} \to 0$. Once $S_I^{inj} = 0$, impurity injection is disabled in subsequent steps by setting $F_{imp} = 0$. By satisfying

$$2\left(S_T^{inj} + S_D^{inj}\right) = -v - K_n \tilde{n}, \quad (48)$$

$$(1-\hat{\gamma}) S_T^{inj} - \hat{\gamma} S_D^{inj} = -\frac{\mathring{n} - 3\mathring{n}_\alpha - (Z_I+1)\mathring{n}_I}{2} K_\gamma \hat{\gamma} - u(\gamma_I^*). \quad (49)$$

We can ensure that $\dot{V}_n < 0$, $\dot{V}_\gamma < 0$, and therefore $\dot{V}_1 < 0$, guaranteeing stability of the system. The conditions (48) and (49) can be satisfied by choosing

$$S_D^{inj} = \frac{\mathring{n} - 3\mathring{n}_\alpha - (Z_I+1)\mathring{n}_I}{2} K_\gamma \hat{\gamma} + u(\gamma^*) + (1-\mathring{\gamma}) \left(\frac{-v - K_n \tilde{n}}{2} \right), \quad (50)$$

$$S_T^{inj} = \left(\frac{-v - K_n \tilde{n}}{2} \right) - S_D^{inj}, \quad (51)$$

which are again subject to saturation. If one of the fueling actuators saturates, we again choose to hold (48).

3.2 Observer Design

The dynamics of the estimation error are governed by

$$\dot{\check{n}}_\alpha = -\tilde{\theta}_1 \frac{\mathring{n}_\alpha}{\tau_E^{sc}} - \theta_1 \frac{\check{n}_\alpha}{\tau_E^{sc}} + L_\alpha, \quad (52)$$

$$\dot{\check{E}} = -\tilde{\theta}_2 \frac{\mathring{E}}{\tau_E^{sc}} - \theta_2 \frac{\check{E}}{\tau_E^{sc}} + L_E, \quad (53)$$

$$\dot{\check{n}}_I = -\tilde{\theta}_7 \frac{\mathring{n}_I}{\tau_E^{sc}} - \theta_7 \frac{\check{n}_I}{\tau_E^{sc}} + L_I, \quad (54)$$

$$\dot{\check{n}}_D = -\tilde{\theta}_3 \frac{\mathring{n}_D}{\tau_E^{sc}} - \theta_3 \frac{\check{n}_D}{\tau_E^{sc}} + \tilde{\theta}_4 \frac{\mathring{n}_T}{\tau_E^{sc}} + \theta_4 \frac{\check{n}_T}{\tau_E^{sc}} + L_D, \quad (55)$$

$$\dot{\check{n}}_T = \tilde{\theta}_5 \frac{\mathring{n}_D}{\tau_E^{sc}} + \theta_5 \frac{\check{n}_D}{\tau_E^{sc}} - \tilde{\theta}_6 \frac{\mathring{n}_T}{\tau_E^{sc}} - \theta_6 \frac{\check{n}_T}{\tau_E^{sc}} + L_T, \quad (56)$$

where $\tilde{\theta}_i = \hat{\theta}_i - \theta_i$ and the estimation errors are denoted by $\check{}$. Taking $\check{x} = \left[\check{n}_\alpha, \check{E}, \check{n}_D, \check{n}_T, \check{n}_I\right]^T$, $L = [L_\alpha, L_E, L_D, L_T, L_I]^T$, $\Theta = \left[\tilde{\theta}_1, \tilde{\theta}_2, \tilde{\theta}_3, \tilde{\theta}_4, \tilde{\theta}_5, \tilde{\theta}_6, \tilde{\theta}_7\right]^T$, this can be written in a more compact form

$$\dot{\check{x}} = A\check{x} + L + \Phi\Theta, \quad (57)$$

where A is negative definite for physically relevant model parameters and

$$\Phi = -\frac{1}{\tau_E^{sc}} \begin{bmatrix} \mathring{n}_\alpha & 0 & 0 & 0 & 0 & 0 & 0 \\ 0 & \mathring{E} & 0 & 0 & 0 & 0 & 0 \\ 0 & 0 & \mathring{n}_D & -\mathring{n}_T & 0 & 0 & 0 \\ 0 & 0 & 0 & 0 & -\mathring{n}_D & \mathring{n}_T & 0 \\ 0 & 0 & 0 & 0 & 0 & 0 & \mathring{n}_I \end{bmatrix}. \quad (58)$$

We consider the Lyapunov function

$$\check{V} = \frac{1}{2}\check{x}^T Q \check{x} + \frac{1}{2}\check{z}^T K_I \check{z}, \quad (59)$$

where Q is positive definite and $\check{z}$ is given by (21). We calculate the time derivative of $\check{V}$ as

$$\dot{\check{V}} = \check{x}^T \left[QA\check{x} + QL + Q\Phi\Theta \right] + \check{z}^T K_I \check{y}. \quad (60)$$

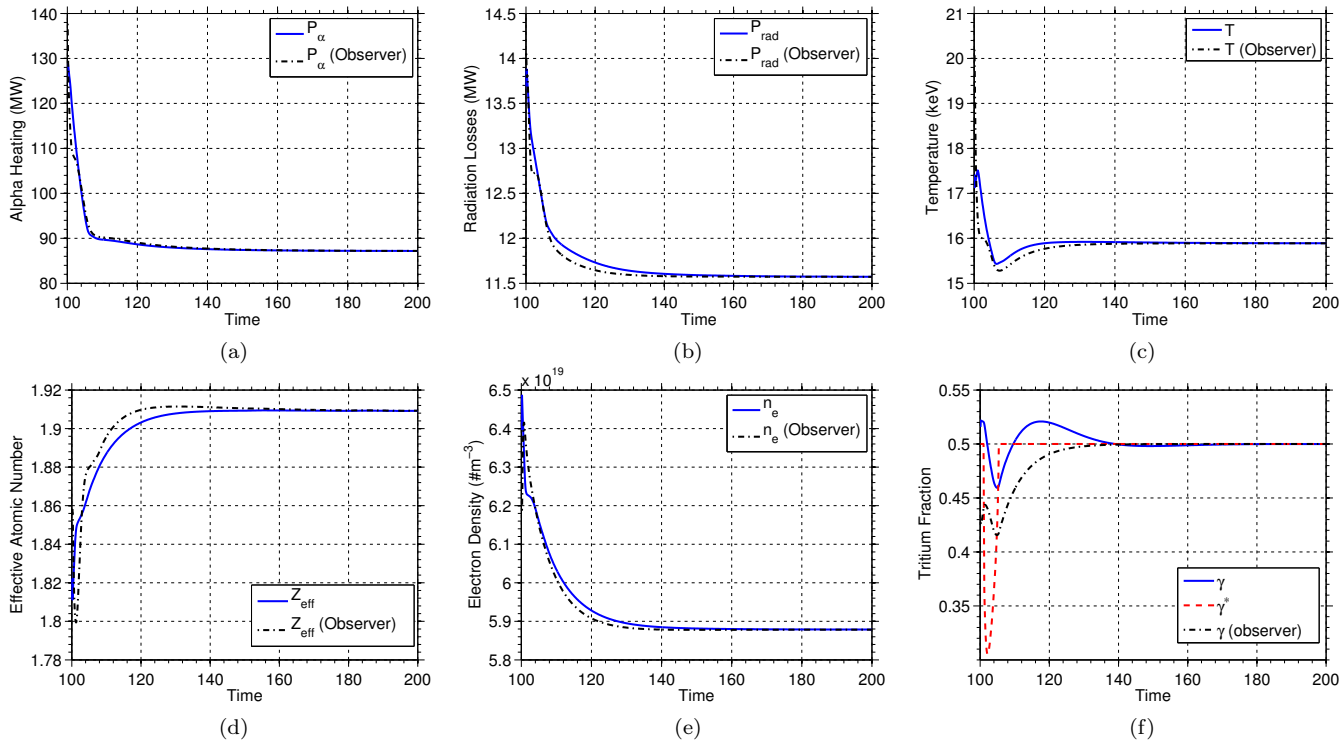

Fig. 1. Comparison of measured outputs to the values calculated from the states of the observer during the output feedback simulation using the uncertain model. The desired tritium ratio, γ^*, is shown in (f).

Noting that the output error can be written as $\check{y} = \left.\frac{\partial h}{\partial x}\right|_{x=\mathring{x}} \check{x} + H.O.T.$ (higher order terms) and that the scalar term $\check{z}^T K_I \check{y}$ is equivalent to $\check{y}^T K_I^T \check{z}$, we can write

$$\dot{\check{V}} = \check{x}^T Q \left[A\check{x} + L + \Phi\Theta + Q^{-1} \left.\frac{\partial h}{\partial x}\right|_{x=\mathring{x}}^T K_I^T \check{z} \right] + (H.O.T.)\, K_I^T \check{z}. \quad (61)$$

By choosing

$$\begin{aligned} L &= -Q^{-1} \left.\frac{\partial h}{\partial x}\right|_{x=\mathring{x}}^T K_I^T \check{z} + A_0 \left.\frac{\partial h}{\partial x}\right|_{x=\mathring{x}}^T \check{y} \\ &= -Q^{-1} \left.\frac{\partial h}{\partial x}\right|_{x=\mathring{x}}^T K_I^T \check{z} \\ &\quad + A_0 \left.\frac{\partial h}{\partial x}\right|_{x=\mathring{x}}^T \left(\left.\frac{\partial h}{\partial x}\right|_{x=\mathring{x}} \check{x} + H.O.T. \right), \end{aligned} \quad (62)$$

where A_0 is a negative definite matrix, we have that

$$\dot{\check{V}} = \check{x}^T Q \left[A\check{x} + A_0 \left.\frac{\partial h}{\partial x}\right|_{x=\mathring{x}}^T \left.\frac{\partial h}{\partial x}\right|_{x=\mathring{x}} \check{x} + \Phi\Theta \right] + QA_0 \left.\frac{\partial h}{\partial x}\right|_{x=\mathring{x}}^T (H.O.T) + (H.O.T.)\, K_I^T \check{z}. \quad (63)$$

If θ is known exactly, then $\Theta = 0$ and $\dot{\check{V}} \leq 0$ for sufficiently small state estimation errors or observer gains. It can be shown that the system is input-to-state-stable with respect to Θ, implying that $\check{x}$ will be bounded for bounded parameter errors. Furthermore, since $\check{z}$ is bounded and $\check{z} = \int_0^t (\mathring{y} - y)\, d\tau$, the estimated and measured outputs converges. This implies that, despite uncertainty in the actual states, if the references E^r, γ^r, and n^r are chosen such that the observer output tracks a desired target, the measured output will converge to that same target.

4. SIMULATION RESULTS

In the following, the nominal model parameters were taken as $\theta_1 = 0.333$, $\theta_2 = 1$, $\theta_3 = 0.1733$, $\theta_4 = 0.0832$, $\theta_5 = 0.0832$, $\theta_6 = 0.1733$, $\theta_7 = 0.1$. As a test of robustness, perturbed parameters were used in the controller and observer design, i.e., $\hat{\theta}_1 = 1.3\theta_1$, $\hat{\theta}_2 = 1.3\theta_2$, $\hat{\theta}_3 = 0.7\theta_3$, $\hat{\theta}_4 = 1.3\theta_4$, $\hat{\theta}_5 = 0.7\theta_5$, $\hat{\theta}_6 = 1.3\theta_6$, $\hat{\theta}_7 = 1.1\theta_7$. The observer gain was designed with $Q = diag(8\text{E-}36, 2\text{E-}38, 2\text{E-}38, 3\text{E-}10, 2\text{E-}36)$, $A_0 = -diag(8,5,5,1,6)$, and $K_I = 0.1 diag(1\text{E-}34, 1\text{E-}6, 0.02, 4.0, 3\text{E-}40, 8)$.

Figure 1 compares the output measurements to the values calculated from the estimated states of the observer. The observed outputs converge to the measured values, and remain close to the measured values throughout the simulation. The states of the system are compared with the estimated states in Figure 2 (a)-(d). As expected, the estimated states converge to the actual values over time. Despite the absence of direct state measurements and uncertain initial conditions, the scheme is able to drive the energy, density, and tritium fraction to their respective desired references. Finally, the controlled actuators are shown in Figure 2 (e) and (f), showing how the isotopic fueling technique was used to account for saturation of the ICRH power early in the simulation.

5. CONCLUSIONS

A nonlinear output feedback control scheme for tracking the burn condition in fusion reactors has been presented. The scheme uses auxiliary heating and fuel in-

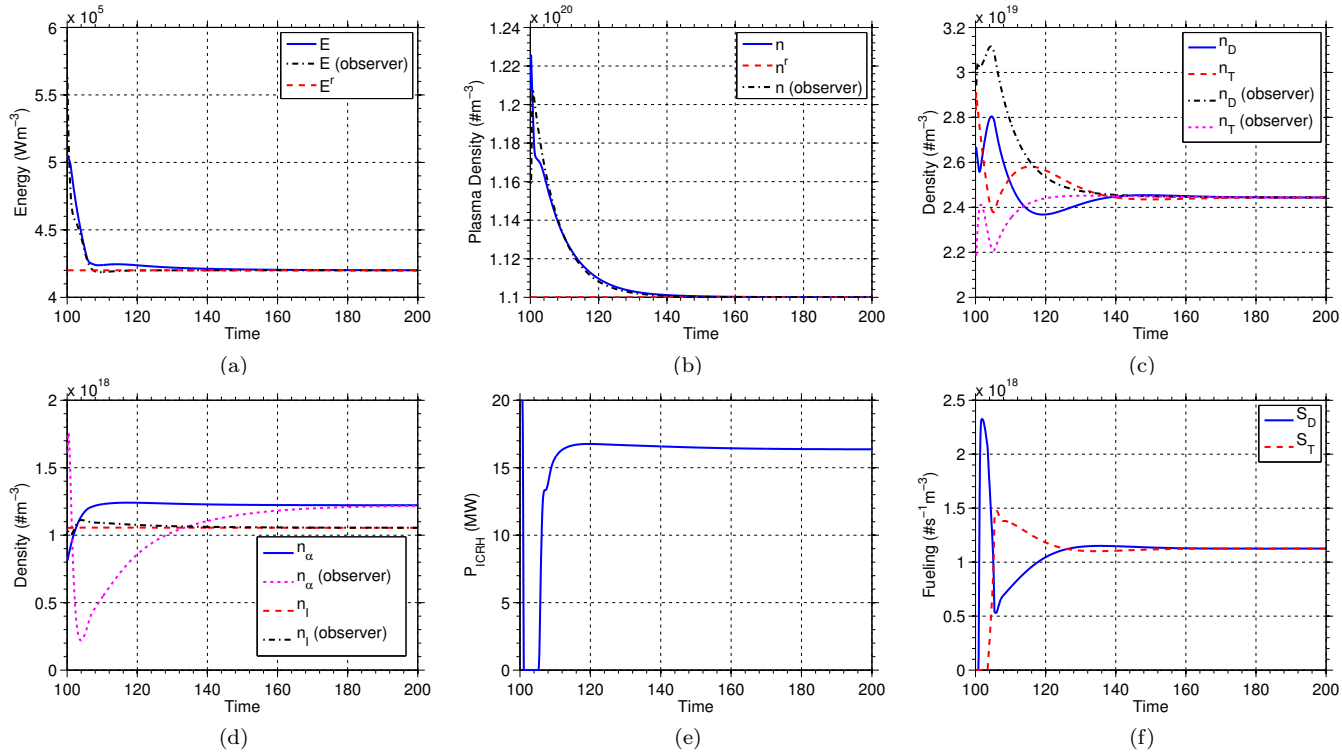

Fig. 2. Comparison of state estimations to actual values ((a)-(d)), as well as control input evolutions ((e)-(f)). Note that $P_{aux} = P_{ICRH} + P_{CD}$, where $P_{CD} = 40$ MW is a fixed power due to non-inductive current drive sources.

jection to stabilize and track desired equilibria (impurity injection is also used, when necessary). The nonlinear proportional-integral observer guarantees the desired outputs are tracked despite model uncertainty. A simulation study shows the performance of the scheme with a set of measurements likely to be available on future reactors. Future work will involve coupling the output feedback controller with online optimization and parameter estimation schemes, and testing the control strategy with other codes like METIS or TRANSP.

REFERENCES

Beale, S. and Shafai, B. (1989). Robust Control System Design with the Proportional Integral Observer. *International Journal of Control*, 50(1), 554–557.

Boyer, M. and Schuster, E. (2011). Zero-dimensional nonlinear burn control using isotopic fuel tailoring for thermal excursions. In *IEEE Int. Conf. Control Applications*, 246–251.

Boyer, M. and Schuster, E. (2012). Adaptive Nonlinear Burn Control in Tokamak Fusion Reactors. In *2012 American Controls Conference*.

Haney, S.W., Perkins, L.J., Mandrekas, J., and Stacey, W.M. (1990). Active Control of Burn Conditions for the International Thermonuclear Experimental Reactor. *Fusion Tech.*, 18(4), 606–17.

Hively, L. (1977). Special Topic Convenient Computational Forms For Maxwellian Reactivities. *Nuclear Fusion*, 17(4), 873.

ITER Director (2001). Summary of the ITER final design report. Technical report, Int. Atomic Energy Agency, Vienna.

Jung, J., Huh, K., and Shim, T. (2007). Dissipative Proportional Integral Observer for a Class of Uncertain Nonlinear Systems. In *2007 American Control Conference*, 269–274. IEEE, New York City, NY.

Leonov, V.M., Mitrishkin, Y.V., and Zhogolev, V.E. (2005). Simulation of Burning ITER Plasma in Multi-Variable Kinetic Control System. In *32nd EPS Conference on Plasma Physics*, volume 29, 2–5.

Mandrekas, J. and Stacey, W.M. (1989). Evaluation of Different Burn Control Methods for the International Thermonuclear Experimental Reactor. *Proc. of the 13th IEEE Symp. on Fusion Engineering*, 1, 404–407.

Mitarai, O. (2002). Fuel Ratio and Fueling Control for Safe Ignited Operation in ITER class Tokamak Reactors. In *Advances in Plasma Physics Research, Vol. 2*, 37. Nova Science Publishers.

Mitarai, O., Sagara, A., Sakamoto, R., and Others (2010). High-Density, Low Temperature Ignited Operations in FFHR. *Plasma and Fusion Research*, 5, S1001–S1001.

Orjuela, R., Marx, B., Ragot, J., and Maquin, D. (2008). Proportional-Integral observer design for nonlinear uncertain systems modelled by a multiple model approach. *47th IEEE Conf. on Decision and Control*, 3577–3582.

Schuster, E., Krstić, M., and Tynan, G. (2003). Burn Control in Fusion Reactors Via Nonlinear Stabilization Techniques. *Fusion Science and Technology*, 43.

Snipes, J., Beltran, D., Casper, T., et al. (2012). Actuator and diagnostic requirements of the ITER Plasma Control System. *Fusion Eng. and Design*, 87(12), 1900.

Stacey, W.M. (2010). *Fusion: An Introduction to the Physics and Technology of Magnetic Confinement Fusion*. Wiley-VCH, Weinheim, 2nd edition.

Vitela, J.E. (2001). Burn Conditions Stabilization with Artificial Neural Networks of Subignited Thermonuclear Reactors with Scaling Law Uncertainties. *Plasma Physics and Controlled Fusion*, 43, 99–119.